

**MINISTRY OF EDUCATION  
AND TRAINING**

**VIETNAM ACADEMY OF  
SCIENCE AND TECHNOLOGY**

**GRADUATE UNIVERSITY OF SCIENCE AND TECHNOLOGY**

---



**Bui Quang Tien**

**FABRICATION AND CHARACTERIZATION OF AN INTEGRATED  
MICROFLUIDIC SYSTEM. ORIENTATION TOWARDS  
APPLICATIONS IN ANALYSIS AND MATERIAL SYNTHESIS**

**SUMMARY OF DISSERTATION ON SCIENCES OF MATTER**

Major: Materials for Electronics

Code: 9 44 01 23

*Hanoi - 2026*

The dissertation is completed at: Graduate University of Science and Technology, Vietnam Academy Science and Technology

Supervisors:

1. Supervisor 1: Prof. Dr. Trần Đại Lâm – Institute of Materials Science, Vietnam Academy of Science and Technology
2. Supervisor 2: Assoc. Prof. Dr. Phan Huy Hoàng – Hanoi University of Science and Technology

Referee 1:.....

Referee 2:.....

Referee 3:.....

The dissertation is examined by Examination Board of Graduate University of Science and Technology, Vietnam Academy of Science and Technology at..... (time, date.....)

The dissertation can be found at:

1. Graduate University of Science and Technology Library
2. National Library of Vietnam

## INTRODUCTION

The outbreak of COVID-19 has demonstrated the need to shift from a centralized healthcare model to distributed, point-of-care diagnostic solutions based on compact devices that remain accurate and sensitive. Hence, POCT systems are receiving strong interest, especially those detecting nucleic acids by electrochemical methods combined with isothermal LAMP amplification, due to their ease of miniaturization, low cost, and suitability for resource-limited settings. Microfluidic technology allows the integration of the entire sample-preparation, amplification, and detection workflow on a single chip, reducing sample volume, shortening assay time, and enabling deployment outside laboratories. In this direction, electrochemical biosensors (particularly immuno- and NA-based sensors) are preferred because of their high sensitivity and selectivity, disposability, and automation potential when integrated with microfluidic chips. Therefore, this research focuses on designing and fabricating a microfluidic device integrated with an electrochemical biosensor, aiming at applications in biomedical testing and point-of-care diagnosis.

### *Thesis objectives*

(1) To fabricate and integrate an electrochemical biosensor with a microfluidic system optimized for LAMP amplification and product detection. (2) To build an electrode-integrated model and study the use of improved peripheral devices to miniaturize the system and reduce sample volume. (3) To develop a label-free electrochemical measurement procedure using a biosensor for detecting biological components, with the ability to be tailored to specific requirements.

### *Approach and research methodology*

Experimental research is the main method of the thesis. The approach consists of examining experimental results to make initial assessments, combining them with theory and reference literature, explaining, comparing, drawing accurate conclusions, and optimizing the experimental protocol.

### *Thesis content*

To achieve the set objectives, the thesis focuses on three main research contents: Content 1: Design and fabrication of an integrated microfluidic device for real-time electrochemical monitoring of nucleic acid amplification by LAMP, using the intercalation between amplified DNA and a free redox probe in the liquid phase. Content 2: Fabrication of an rGO-PANi sensor to monitor pH changes during LAMP; an rGO film is produced by electrochemical reduction of graphene oxide, followed by PANi electrodeposition, and open-circuit potential measurements are used to detect amplified DNA. Content 3: Design and optimization of a microfluidic system integrating electrodes, a heater, and microchannels for LAMP and electrochemical detection; this includes channel simulation, Pt heater simulation, and device fabrication aiming at a point-of-care testing device.

### *Scientific and practical significance*

The thesis aims at a miniaturized, low-cost analytical platform that maintains high sensitivity and selectivity, shortens analysis time, and reduces sample volume, suitable for deployment in areas lacking centralized testing facilities. A PDMS microfluidic system integrated with an electrochemical biosensor is used to monitor the LAMP reaction, with cyclic voltammetry and amperometry techniques employed to investigate electrochemical properties.

### *New contributions*

The thesis has designed and fabricated a small-scale reaction channel system integrated with an electrode array that can be directly connected to a readout circuit, thereby reducing sample volume and improving the signal-to-noise ratio. The combination of microfluidics with conductive materials such as graphene, polyaniline, 2D materials, and metal nano-materials allows both on-chip material synthesis and their use as sensing electrodes or functional elements – a research direction still novel in Vietnam.

### *Layout and publications*

The thesis comprises 101 pages (excluding table of contents and references), consisting of an Introduction; Chapter 1 – Literature Review; Chapter 2 – Materials and Methods; Chapter 3 – Results and Discussion; and a Conclusion section. The main results have been published in 5 scientific works, including 4 ISI journal papers and 1 international conference report.

## CHAPTER 1. LITERATURE REVIEW

### 1.1. Biochip and Microfluidics

Biochips and microfluidic systems allow the miniaturization of the entire analytical process – from sample preparation, reaction, to signal detection – onto a microscale platform, overcoming the time, cost, and infrastructure limitations of conventional diagnostic techniques such as culture, PCR, or ELISA. Biochips integrate active biological elements (DNA, antibodies, enzymes, etc.) on a solid support and can perform thousands of reactions simultaneously, finding wide application in agriculture, food safety, environmental monitoring, biosecurity, and especially personalized medicine. Microfluidics, based on micrometer-sized channels with laminar flow and microscale effects (capillarity, electroosmosis, diffusion, etc.), allows precise manipulation of extremely small liquid volumes and acts as an optimal “micro-reactor” for material synthesis and processing, particularly for nanoparticles, owing to excellent control over residence time and thermal/concentration gradients.

In terms of fabrication, early generations using glass/silicon are gradually being replaced by polymers such as PDMS, PC, PMMA, and even nitrocellulose paper, reducing cost and increasing flexibility; current trends involve multi-material combinations and the use of 3D printing to create complex architectures. Integrated microfluidic-biochip systems (lab-on-a-chip) have demonstrated their effectiveness in POCT: automating lysis, extraction, amplification (PCR, LAMP), and detection (electrochemical, fluorescence, plasmonic) on a small chip, as exemplified by GeneXpert or RT-LAMP chips for SARS-CoV-2 detection with greatly reduced sample volume and assay time compared to tube-based PCR. Nevertheless, the technology still faces challenges such as matrix effects from complex biological samples, non-specific adsorption on PDMS, gas permeability affecting enzyme activity, batch-to-batch variation, and mass-production costs. Future development directions focus on optoelectronic hybrid chips, AI-driven data analysis, organ-on-a-chip models, and multi-material 3D printing for next-generation microdevices.

## **1.2. Electrochemical biosensors**

### ***1.2.1. Classification of biosensors***

Electrochemical biosensors are the core of analytical microfluidic systems because microelectrodes (gold, carbon, ITO, or screen-printed electrodes) integrated directly into the channels allow current, potential, or impedance measurements with very small sample volumes and in real time. Owing to their micro-scale dimensions, thin diffusion layers, and short diffusion paths, microelectrodes provide high signal-to-noise ratios and fast responses, while being easily coupled with portable readout circuits (mini potentiostats, NFC, Bluetooth) to form mobile lab-on-a-chip systems.

Biosensors can be divided into three main categories based on the transduction mechanism: optical (e.g., SPR), magnetic (based on magnetic nanoparticles), and electrochemical; among these, electrochemical ones are widely used due to low cost, easy miniaturization, and suitability for complex samples. Electrochemical biosensors employ a biological recognition element (enzyme, antibody, aptamer, DNA) immobilized on the working electrode, converting the biological interaction into a current, potential, or impedance signal, measured by amperometry, potentiometry, or EIS. Performance and technique choice depend on sensitivity, limit of detection, device size/portability, sample pretreatment level, response time, and overall cost; in the POCT context, electrochemical biosensors are outstanding because of the availability of low-cost, disposable screen-printed electrodes that can be integrated with microfluidics and mobile devices.

### ***1.2.2. Electrochemical analysis***

Electrochemical analysis in general relies on a three-electrode system (WE, RE, CE) and a potentiostat that controls the potential and records the current; biological interactions alter the faradaic current or impedance at the WE, thereby quantifying the analyte concentration. In recent years, the number of publications on electrochemical analysis and electrochemical biosensors has grown very rapidly, especially with nanomaterials (graphene, MXene, nanocomposites) and microfluidic integration, demonstrating great potential for next-generation biomedical diagnosis, disease monitoring, and environmental sensing.

### ***1.2.3. Measurement techniques in electrochemical biosensing***

The measurement techniques in electrochemical biosensing can be briefly summarized as follows:

Many methods exist, but the thesis focuses on three main techniques: CV, EIS, and DPV for detecting nucleic acid amplification products.

CV scans the potential in a triangular waveform and records the current, producing a voltammogram with oxidation/reduction peaks; the height and position of the peaks reflect the concentration and reversibility of the redox indicator (e.g., MB,  $\text{Fe}(\text{CN})_6^{3-/4-}$ ), which is very useful for investigating electrode surface changes and reaction mechanisms.

EIS applies a small AC perturbation around a fixed DC potential, measures the impedance as a function of frequency, and models it with an equivalent circuit; the most important parameter is the charge-transfer resistance  $R_{ct}$ , which increases when the surface is coated or DNA is hybridized, enabling label-free detection down to the fM range.

DPV uses small potential pulses superimposed on a scanned potential and measures the difference in current before and after each pulse to eliminate almost all capacitive current, yielding sharp and sensitive peaks suitable for quantifying redox indicators related to DNA at very low concentrations.

Choosing and optimizing each technique (potential range, pulse amplitude and duration, AC amplitude, frequency, etc.) is critical to achieving the desired sensitivity, accuracy, and limit of detection in electrochemical nucleic acid biosensor design.

### ***1.2.4. Electrochemical sensors integrated with microfluidic devices***

In biosensing, integrating electrodes into a microfluidic chip allows the entire analytical procedure (sample loading, processing, signal measurement) to be performed on a single compact platform, reducing sample volume, shortening time, and increasing sensitivity; common structures include microchannel-based and paper-based microfluidics, which can use continuous flow or discrete droplets to minimise cross-contamination. Electrodes can be fabricated in-situ by sputtering/photolithography or attached externally, offering design

flexibility and lowering mass-production costs, while also enabling the integration of sample-preparation modules (microfiltration, cell sorting by diffusion or dielectrophoresis) and passive (capillary) or active (pump, manual press) flow control mechanisms.

### ***1.2.5. Domestic research status of electrochemical sensors integrated with microfluidics***

In Vietnam, research on electrochemical biosensors is mainly carried out by groups at Hanoi University of Science and Technology, VNU-HCM, the Institute of Materials Science, and some other universities/institutes, with many sensor systems based on interdigitated electrodes or nanomaterials for detecting pesticides, heavy metals, glucose, cholesterol, cancer markers, HIV, aflatoxin, and DNA/viruses. However, integrated microfluidic-electrochemical systems are still very rare; only a few initial works have fabricated paper- or PDMS-based microchannels combined with sensors for ELISA or DNA detection, indicating that this is a new research direction with much room for development in the country.

### **1.3. Loop-mediated isothermal amplification (LAMP)**

Nucleic acid amplification is a key platform for detecting microorganisms due to its high selectivity and sensitivity, with two main approaches: PCR and isothermal amplification methods. PCR uses a three-temperature cycle (denaturation – annealing – extension) with a heat-stable enzyme such as Taq, allowing up to billions of copies of the target gene, but requires expensive thermal cyclers, many auxiliary instruments, and is difficult to deploy outside laboratories.

Isothermal amplification techniques, notably LAMP and RPA, overcome this limitation by performing the reaction at a constant temperature around 60–65 °C, requiring simpler energy sources and instrumentation. In LAMP, an enzyme such as Bst/Bsm polymerase with strand-displacement activity works with 2–3 primer pairs recognizing 6–8 regions on the target gene, generating a very large amount of double-stranded DNA in only 40–60 minutes. The products have a looped/ladder structure and can be detected directly by eye using intercalating dyes without electrophoresis. Hence, LAMP has a lower detection limit than PCR/RT-PCR, a shorter reaction

time, a lower risk of cross-contamination because amplification and reading occur in a single tube, and can be extended to RNA amplification by adding reverse transcriptase; these features make LAMP particularly suitable for field testing and infrastructure-poor settings.

### ***1.3.1. Principle of LAMP***

LAMP uses 4–6 special primers recognizing 6–8 regions on the target DNA, together with Bst polymerase, to amplify DNA at a constant temperature of 55–65 °C with very high efficiency (up to 10<sup>9</sup>–10<sup>10</sup> copies in 15–60 minutes).

### ***1.3.2. Basic components of LAMP reaction***

The reaction mixture contains template DNA (not requiring high purity), LAMP primers, dNTPs, buffer, and indicator dyes (SYBR Green, HNB, calcein, malachite green, etc.) to observe products directly through turbidity or color change.

### ***1.3.3. Mechanism of LAMP***

The mechanism consists of three stages: formation of a “stem-loop DNA” from the target gene, a cycle of replication and extension using the FIP/BIP primers on the loop structure, and repeated cycling to produce a mixture of bent-loop DNA with very large lengths.

### ***1.3.4. Advantages and disadvantages of LAMP***

The outstanding advantages of LAMP are that it does not require expensive thermal cyclers, only a stable heat source; the reaction is isothermal, assay time is short, sensitivity and specificity are high, results can be read by the naked eye, and simple DNA extraction is acceptable. Disadvantages include the need for nucleic acid extraction, high susceptibility to cross-contamination due to its high sensitivity, and higher cost compared to morphological methods or ELISA.

In Vietnam, LAMP and RT-LAMP have been applied to rapidly detect many pathogens in livestock, plants, and human health (*E. coli* O157:H7, white spot disease in shrimp, *Phytoplasma* in cassava, citrus greening, rabies virus, Japanese encephalitis, Dengue, etc.). Some have been developed into commercial kits, such as LAMP kits for shrimp viruses and in-house RT-LAMP kits for Dengue.

### ***1.3.5. Integration of LAMP into microfluidic devices***

Integrating LAMP into microfluidic devices allows sensitive and specific nucleic acid amplification without thermal cyclers, making it highly suitable for point-of-care diagnosis. Many platforms have been developed, from microchannel chips with magnetic-bead DNA extraction to “sample-in-answer-out” systems integrated into micropipette tips, where extraction, amplification, and fluorescence reading all occur in a very small volume. Other innovative solutions use RT-LAMP combined with chemical heating and lateral-flow strips or commercial pregnancy test strips to detect HIV-1 or SARS-CoV-2 without electricity, reading results by eye through the appearance/disappearance of a line on the strip. Besides qualitative detection, LAMP has also been implemented as “digital LAMP” in water-in-oil droplets for absolute quantification of drug-resistance genes, as well as on paper devices measuring the length of a colour bar as a function of DNA concentration, enabling semi-quantitative pathogen detection with low-cost, disposable, and highly portable configurations.

Based on the literature review of electrochemical biosensor research worldwide and in Vietnam, several key research directions can be identified:

The first direction focuses on designing and fabricating electrode systems, because the electrode material (Au, Pt, various forms of carbon) and fabrication technology directly determine the sensitivity, cost, and ability to immobilize biological recognition elements on the sensor surface. The second direction is the integration of electrochemical sensors with microfluidic/micro-reactor systems to miniaturize the device, reduce sample volume, improve the signal-to-noise ratio, and move towards portable analysers for field use; this is an international trend but still quite new in Vietnam. The third direction is the development of specific electrochemical measurement procedures for different target biomolecules, optimising the measurement techniques in complex sample matrices as a basis for dedicated devices. Effective implementation of these three directions requires interdisciplinary collaboration among chemistry, physics, electronics, biology, and materials science, in line with the global trend of integrated electrochemical-microfluidic device research.

## CHAPTER 2. MATERIALS AND METHODS

### **2.1. Objective 1: Fabrication of an electrochemical biosensor on a microfluidic system using methylene blue as a redox probe for HBV detection**

#### ***2.1.1. Research objective***

Accurate point-of-care diagnostic tests play a critical role in patient management and the control of most infectious diseases. To achieve this, using a single hand-held bio-device that performs sample processing, analysis, and readout is an ideal approach. In this research content, the thesis aims to design and fabricate an integrated microfluidic device for real-time electrochemical monitoring of nucleic acid amplification by LAMP. The intercalation between amplified DNA products and a free redox probe in the liquid phase is used to follow the number of DNA copies. The entire diagnostic process is completed within 70 minutes.

#### ***2.1.2. Materials and methods***

##### ***2.1.2.1. Materials and chemicals***

Methylene blue (MB), phosphate-buffered saline (PBS) prepared and diluted with ultrapure water (18.3 M $\Omega$ ), Loopamp DNA amplification kit, polydimethylsiloxane (PDMS), and screen-printed electrochemical sensors (AC1.RS1).

##### ***2.1.2.2. Sample preparation and DNA extraction***

Clinical samples (blood samples) were collected from in-patients suspected of HBV infection admitted to the National Hospital of Tropical Diseases (NHTD) in August 2015. All samples had been previously tested at the hospital to obtain an initial positive/negative status. Blood and serum samples were stored at  $-20\text{ }^{\circ}\text{C}$  until analysis. Viral DNA was extracted from 50  $\mu\text{L}$  of serum using a QIAmp DNA mini kit (QIAGEN GmbH, Germany) according to the manufacturer's instructions. DNA was eluted in 50  $\mu\text{L}$  of DNase-free water.

### 2.1.2.3. Fabrication procedure

**Table 2.1. List of primer sequences designed for LAMP**

F3	TCAACCCCATCAAGGACCA
B3	GCCTGAGGATGACTGTCTCT
FIP	CCAAAACACCGCCGTGTGGAAGCCAACC AGGTAGGAGTG
BIP	CAGGCTCAGGGCATGTTGACCTAGGCTGCC TTCCTGACT
LF	AACCCTGGCCCGAATGCTC
LB	GTCAACAATTCCTCCTCCTGCC

### 2.1.2.4. Design and fabrication of the microfluidic device integrated with electrochemical sensor

The LAMP-EC-MF microfluidic device was designed with the following main features: (1,4) inlet and outlet, (2) reaction chamber, and (3) sensor. The rectangular reaction chamber had a volume of 20  $\mu\text{L}$  (Fig. 2.2).

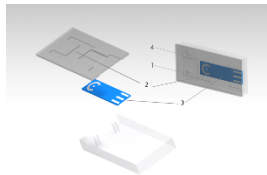


Fig. 2.2. Conceptual design of the LAMP-EC-MF slip-chip.

### 2.1.3. Research content

#### 2.1.3.1. Experiment

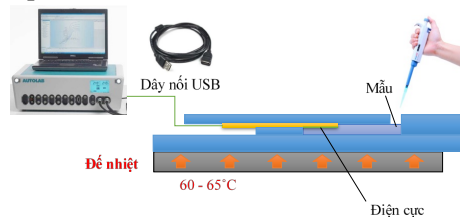


Fig. 2.3. Illustration of the experimental setup for real-time monitoring of HBV DNA amplification.

Measurements were repeated at least twice to confirm reproducibility. The quantitative detection results were then validated by agarose gel electrophoresis and fluorescence assays.

#### *2.1.3.2. Gel electrophoresis*

5  $\mu$ L of LAMP amplification product were stained with (NEB, USA) and 19 mM Tris-borate-EDTA (TBE) buffer (pH 8.0). A 2% agarose gel was stained with Safe-T-Stain, and after running the gel, images were captured for reference.

#### *2.1.3.3. Fluorescence detection*

1  $\mu$ L of Loopamp fluorescent detection reagent was added to 25  $\mu$ L of LAMP product. The mixture was then observed under UV light at 260 nm.

#### *2.1.3.4. Techniques used in the study*

(1) Square-wave voltammetry (SWV) was chosen to monitor the MB redox current during LAMP reactions because of its fast measurement time (under 4 s). SWV parameters: pulse amplitude 1 mV, frequency 12.5 Hz, pulse width 5 mV, using an Autolab instrument (PGSTAT N 32, Metrohm, The Netherlands). (2) Primer design used bioinformatics software such as Primer Explorer v.5, Primer Blast, and Mega 7 to identify conserved regions on target genes, design primers, and check oligonucleotide properties. (3) Sample processing and DNA extraction: combined mechanical grinding, heating, enzymatic digestion, and DNA purification using spin-columns or magnetic beads. (4) Electrophoresis on 2% agarose gel for 30 min at 100 mA.

## **2.2. Objective 2: Fabrication of an rGO - PANi electrochemical sensor for detection of amplified DNA products by open-circuit potential measurement**

### *2.2.1. Research objective*

Recently, the pH decrease caused by pyrophosphate protons released during the LAMP reaction has also been used as an indicator for electrochemical analysis of post-amplification products. After literature

survey, in this next content the thesis will describe the use of pH-sensitive PANi and highly conductive rGO films to fabricate a device that monitors pH changes during gene amplification throughout the LAMP reaction.

## **2.2.2. Materials and methods**

### *2.2.2.1. Chemicals*

Graphene oxide (GO) was prepared from graphite powder; aniline ( $C_6H_5NH_2$ ); PBS buffer (pH 7.4) used as supporting electrolyte; screen-printed carbon electrodes (SPE); Loopamp DNA amplification kit; a set of six primers designed to be compatible with the LAMP kit.

### *2.2.2.2. Preparation of rGO/PANi films\**

The pH-sensitive rGO-PANi sensor was prepared on an SPE. First, graphene oxide ( $1 \text{ mg mL}^{-1}$ ) was drop-cast onto the electrode. Next, the film was electrochemically reduced by cyclic voltammetry scanning from 0 V to 1.2 V for several cycles. Finally, polyaniline was electrodeposited by scanning the SPE || rGO electrode in 0.5 M  $H_2SO_4$  containing 0.3 M aniline for 10 cycles from  $-200 \text{ mV}$  to  $+900 \text{ mV}$ . Surface morphologies were characterized using a Hitachi S-4800 field-emission scanning electron microscope (FE-SEM) at 5 kV. Attenuated total reflection Fourier-transform infrared (ATR-FTIR) spectra were recorded with an IR-Tracer 100 (Shimadzu, Japan) in the range  $500\text{--}4000 \text{ cm}^{-1}$ . The crystallinity of the prepared samples was determined by Raman spectroscopy in the range  $300\text{--}3500 \text{ cm}^{-1}$  using a 532 nm excitation source on a Horiba spectrometer.

### *2.2.2.3. pH testing*

pH calibration measurements were performed using PBS buffers adjusted to pH values from 6.0 to 9.0. These buffers were used to measure the open-circuit potential (OCP) change of the working electrode relative to an Ag/AgCl reference electrode as a function of pH. All experiments were carried out at room temperature. All measurements were performed on a Metrohm Autolab PGSTAT 302N controlled by a computer (Metrohm Co., Ltd., Switzerland).

#### *2.2.2.4. LAMP reaction*

The LAMP mixture was prepared as described in our previous work. Phage DNA was diluted with PBS (pH 7.4) to a concentration of  $10 \text{ ng } \mu\text{L}^{-1}$ .

The reaction mixture (25  $\mu\text{L}$ ) consisted of 1.6  $\mu\text{M}$  FIP and BIP primers, 0.8 mM outer primers (F3 and B3), 0.8 mM loop primers (LPF and LPB), reaction mix (12.5 mL), Bst DNA polymerase (1  $\mu\text{L}$ ), and 5  $\mu\text{L}$  of sample. LAMP was performed at 65 °C and then stopped at 84 °C after various time intervals (0, 10, 20, 30, 40, 60 min). The amount of amplified amplicon was recorded using OCP measurements, where no current flows in the electrochemical cell. LAMP products were also qualitatively analysed by electrophoresis on 2% agarose gels. The exact DNA concentration at each reaction step was determined using a Nanodrop to purify the DNA solution.

#### *2.2.4. Techniques used in the study*

1. Electrochemical reduction by cyclic voltammetry from 0 V to 1.2 V.
2. Polyaniline electrodeposition on the surface by scanning the SPE || rGO electrode in 0.5 M  $\text{H}_2\text{SO}_4$  containing 0.3 M aniline for 10 cycles from  $-200 \text{ mV}$  to  $+900 \text{ mV}$ .
3. Examination of electrode morphology using scanning electron microscopy, Raman spectroscopy, and Fourier-transform infrared spectroscopy.
4. pH response of the rGO/PANi film tested by measuring OCP at different pH values (6.0–9.0).

### **2.3. Objective 3: Design and fabrication of a microfluidic system integrated for LAMP reaction and solution-phase electrochemical detection**

#### *2.3.1. Research objective*

In this chapter, the requirements and specifications of the device for point-of-care testing are listed. Based on that, a suitable microfluidic device design is proposed. The device comprises three parts: microchannels, an electrochemical sensor, and a heater.

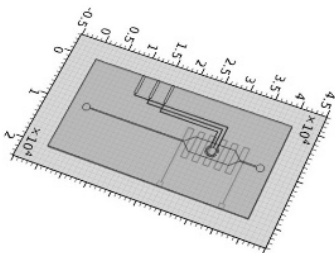


Fig. 2.6. Design of the integrated microfluidic device.

### **2.3.2. Materials and methods**

The device is designed to hold a small amount of sample and LAMP kit mixture in a closed reaction chamber during heating. On a glass substrate, a heating layer and an electrode are separated by a thin insulating layer. The heater is designed to provide sufficient heat to the reaction chamber and to ensure uniform temperature distribution. The insulating layer is spin-coated onto the glass substrate and the resistive heater using polysilazane as the material.

The design and fabrication of PDMS microchannels by photolithography includes the following steps: (i) photomask design; (ii) master fabrication on a silicon wafer; (iii) fabrication of the microchannel system in PDMS by replica moulding.

### **2.3.3. Research content**

#### *2.3.3.1. Photomask design*

AutoCAD 2007 software was used to design the details and geometry of the microchannel system. The design was then transferred to a computer connected to a printer. The designs were printed on high-transmittance material (PET film) as shown in the figure above. Finally, the photomasks were kept clean before being transferred to the photolithography system.

#### *2.3.3.2. Master fabrication for microchannel system*

The master fabrication process was performed according to the steps below, all carried out in a clean room (Takamura Laboratory, Materials

Science School, JAIST): Step 1: Cleaning the silicon wafer; Step 2: Spin-coating SU-8 photoresist to the desired thickness; Step 3: Soft baking; Step 4: Photolithography; Step 5: Post-exposure baking; Step 6: Development with SU-8 developer; Step 7: Rinsing and drying; Step 8: Hard baking to complete the master.



Fig. 2.10. One of the masks containing positive (raised) channel details fabricated by photolithography.

#### 2.3.3.3. *Fabrication of microchannels in PDMS*

PDMS preparation: PDMS and Sylgard 184 curing agent were mixed in a 10:1 ratio, stirred thoroughly, and then degassed under vacuum to remove bubbles. The master was placed in a circular tray. The PDMS mixture was poured over the master. The tray was placed in an oven and heated at 120 °C for 2 h, after which the cured PDMS was peeled off the master, yielding PDMS with the designed microchannel features. The PDMS was washed with isopropanol (or ethanol) and deionised water, then dried with a nitrogen gun. Both the PDMS and the glass slide were treated in a SAMCO Model FA-1 plasma cleaner. After the plasma program finished, the PDMS and glass slide were taken out and bonded together.

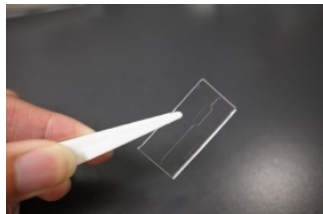


Fig. 2.11. One of the microfluidic systems fabricated in PDMS.

#### 2.3.3.4. Master fabrication for electrodes and heater

The same procedure as described above was followed.

#### 2.3.3.5. Fabrication of gold electrodes and platinum heater

- Heater fabrication: A titanium adhesion layer was deposited first, followed by sputtering of a platinum layer onto the substrate surface. Deposition parameters: Plasma: RF = 120 W, 31 sccm Ar; Ti layer: RF = 75 W, 5.2 sccm Ar, 8 min; Pt layer: RF = 100 W, 4.8 sccm Ar, 10 min.
- Gold electrode fabrication: A titanium layer was deposited first, followed by sputtering of a gold layer onto the substrate surface. Layer thicknesses: Au 50 nm, Ti 5 nm. Deposition parameters: Ti layer: 0.02 nm/s, 11.3 A, 40 mA, 5 min; Au layer: 0.06 nm/s, 12 A, 80 mA, 15 min.

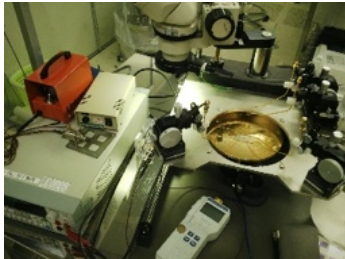


Fig. 2.18. Testing the heater performance with a four-point probe system.

The heater was supplied with a defined current by a source meter, and the temperature was measured at several arbitrary points on the heater.

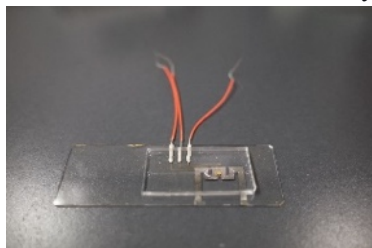


Fig. 2.19. The fully assembled microfluidic device integrating electrodes and a heater.

## CHAPTER 3. RESULTS AND DISCUSSION

### 3.1. Fabrication of an electrochemical biosensor on a microfluidic system using methylene blue as a redox probe for HBV detection

#### 3.1.1. Results and discussion

##### 3.1.1.1. Electrochemical stability of the redox probe

A 20  $\mu\text{M}$  MB solution was heated at 60–65  $^{\circ}\text{C}$ . After 30 min, no change in the output signal was observed; the signal remained around 1.1  $\mu\text{A}$  ( $\pm 5\%$ ), confirming that subsequent real-time HBV quantification experiments using methylene blue interaction could be carried out.

##### 3.1.2. Real-time HBV detection

The real-time redox current data showed a clear decrease during the 30 min reaction (Fig. 2.5). At the start of the reaction, a relatively high redox current (1.3  $\mu\text{A}$ ) was obtained due to free MB molecules in solution.

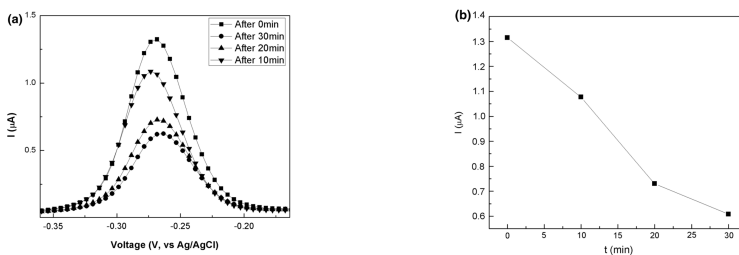


Fig. 3.2. Real-time HBV detection on the LAMP-EC-MF system.

At the end of the reaction, the binding of MB to the dsDNA amplicons produced by LAMP significantly reduced the free MB concentration in the sample solution, thereby decreasing the peak current to 0.6  $\mu\text{A}$ .

##### 3.1.3. Comparison with gel electrophoresis and fluorescence

The gel electrophoresis image (Fig. 2.6) showed multiple bands of different sizes for the positive sample, and a bright fluorescence signal (Fig. 2.7) was also obtained for the positive sample, consistent with the results from the device.

### 3.1.4. Conclusion

The integrated LAMP-electrochemical-microfluidic device allows pathogen detection from a very small sample volume in less than 70 min, significantly faster than conventional PCR while maintaining high sensitivity and specificity. The simple microfluidic design, low reaction temperature, and on-chip electrochemical measurement make the system suitable for development as a handheld device for screening HBV and other pathogens at the point of care, especially in resource-limited settings.

## 3.2. Fabrication of an rGO-PANi electrochemical sensor for detection of amplified DNA products by open-circuit potential measurement

### 3.2.1. Results and discussion

#### 3.2.1.1. Preparation of the rGO-PANi film

The rGO-PANi film was prepared by electropolymerisation of aniline (0.3 M) in 0.5 M H<sub>2</sub>SO<sub>4</sub> on the surface of an SPE modified with rGO.

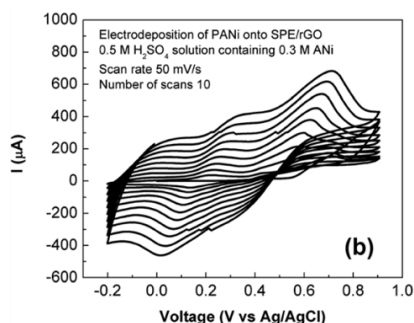


Fig. 3.7. Electrodeposition of polyaniline onto SPE/rGO.

As seen from Fig. 3.1, a strong reduction peak appeared at about -1000 mV with an onset potential of -900 mV in the first cycle of the cyclic voltammogram of graphene oxide, indicating the reduction of the drop-cast GO. In subsequent cycles, the intensity of the reduction peak dropped sharply (Fig. 3.2). Meanwhile, no anodic peak was observed for all cycles. This demonstrates an irreversible conversion in which graphene oxide is

completely reduced to its reduced form. The cyclic voltammograms recorded during PANi deposition on the rGO film are shown in Fig. 3.7.

The continuous increase in current density indicated the growth of PANi on the rGO surface. The transitions between different oxidation states of polyaniline were also observed during deposition. As seen in the CVs in Fig. 3.3, the first anodic wave at +225 mV (vs. Ag/AgCl) corresponds to the conversion of leucoemeraldine to emeraldine salt, while the second anodic wave at +565 mV (vs. Ag/AgCl) indicates the formation of fully doped pernigraniline salt. The final scan was stopped at 0 V to obtain emeraldine – the only conducting form of polyaniline.

### 3.2.1.2. Structure and morphology of the rGO-PANi film

The ATR-FTIR spectrum of rGO recorded the presence of C=C stretching ( $1400\text{--}1600\text{ cm}^{-1}$ ), the disappearance of  $\text{C=O}$  ( $1700\text{ cm}^{-1}$ ) and  $\text{C-O}$  ( $1010\text{ cm}^{-1}$ ) stretching of carboxylic and epoxide groups. This indicates that most of the oxygen-containing groups on the drop-cast graphene oxide had been removed. Simultaneously, characteristic bands of the emeraldine structure were clearly observed on the electrodeposited rGO/PANi film:  $1564$  and  $1491\text{ cm}^{-1}$  (C=C stretch),  $1298\text{ cm}^{-1}$  (C-N stretch),  $1134\text{ cm}^{-1}$  (C=N),  $797\text{ cm}^{-1}$  (C-H).

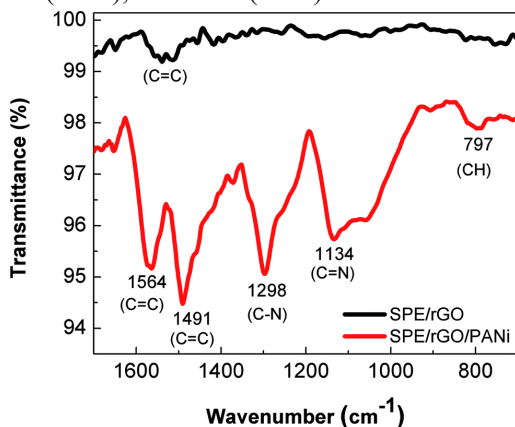


Fig. 3.10. ATR-FTIR spectra of rGO (black) and rGO-PANi (red) films.

Fig. 3.10 shows the Raman spectra of the rGO and rGO-PANi films. The peaks at  $1335\text{ cm}^{-1}$ ,  $1581\text{ cm}^{-1}$ , and  $2686\text{ cm}^{-1}$  are assigned to the typical D, G, and 2D bands of graphitic materials, respectively. The D band is related to defects, edges, and structural disorders of solid carbon, while the G band is associated with first-order scattering of the  $E_{2g}$  mode of  $sp^2$ -hybridised carbon. The intensity ratio  $I_D/I_G$  is an effective indicator of the conversion between GO and rGO. Here, the Raman spectrum (Fig. 3.11) of rGO after electrochemical reduction showed an  $I_D/I_G$  ratio of 0.946, significantly higher than the value of 0.803 for GO.

This indicates an increase in the number of defect sites due to the removal of functional groups from GO and the electroreduction of GO to rGO. When polyaniline was electrodeposited on rGO, the positions of the above peaks (Fig. 3.11) shifted slightly to higher wavenumbers:  $1337\text{ cm}^{-1}$ ,  $1585\text{ cm}^{-1}$ , and  $2760\text{ cm}^{-1}$ . Other Raman peaks at  $812$ ,  $1164$ ,  $1244$ ,  $1403$ ,  $1483\text{ cm}^{-1}$  correspond to amine deformation (benzoid), in-plane C–H bending (benzoid), C–N<sup>+</sup> stretching of open-chain amine (quinoid), C–C stretching (quinoid), and N–H bending (quinoid), respectively (Fig. 3.11).

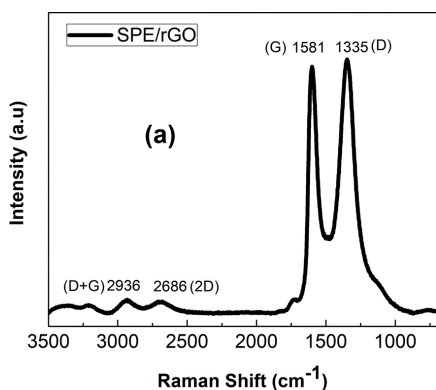


Fig. 3.11. Raman spectrum of rGO film.

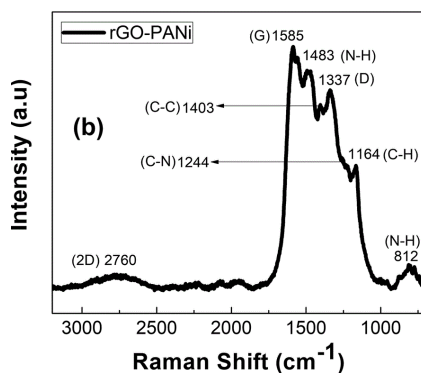


Fig. 3.12. Raman spectrum of rGO-PANi film.

### 3.2.1.3. pH testing

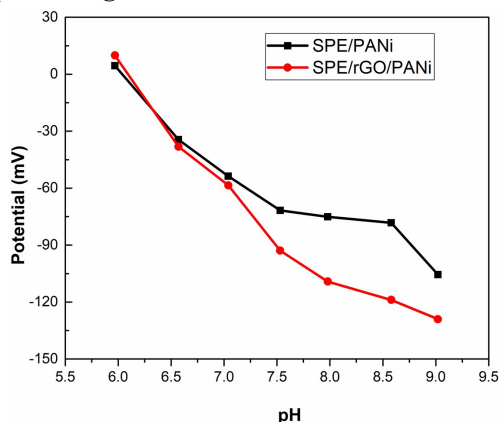


Fig. 3.14. pH calibration curves of SPE/PANi (black) and SPE/rGO-PANi (red).

Depending on the electrode fabrication process, the slope of the calibration curve lies in the range of 55–90 mV per pH unit. Compared to the pristine polyaniline film (Fig. 3.8), the rGO-PANi composite exhibited a larger slope of the OCP-pH response curve, which can be attributed to the high electrical conductivity of the rGO material.

### 3.2.1.4. LAMP reaction

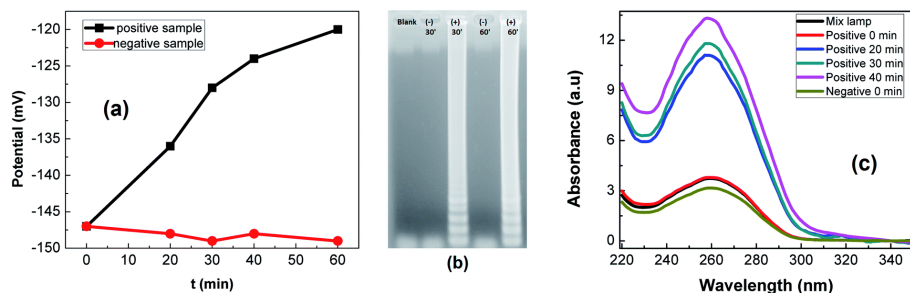


Fig. 3.15, 3.16, 3.17. LAMP reaction: OCP detection (a), gel electrophoresis (b), and absorbance measurement (c) of LAMP products.

The detection mechanism relies on the pH decrease caused by hydronium ions released during DNA elongation in the LAMP reaction.

Fig. 3.10(a) shows the normalised potential change measured during the LAMP reaction for positive and negative samples. The OCP value increased with reaction time (27 mV over 40 min), indicating an increase in the number of amplicons and released protons. In contrast, a negligible OCP decrease was found for the negative sample (Fig. 6(a)). This demonstrates the high specificity of the sensor. These results correlate well with gel electrophoresis and absorbance measurements. In Fig. 3.10(b), the positive LAMP sample showed multiple bands of different sizes on the agarose gel. Simultaneously, the DNA concentration was found to increase by about  $10^3$ -fold (as determined from the absorption spectra (Fig. 3.10(c))).

### **3.2.2. Conclusion**

The pH sensitivity of rGO-PANi was successfully studied and applied to detect the LAMP reaction by OCP measurement. The rGO adsorption layer, with its high conductivity and intrinsic pH sensitivity, contributed to the overall enhanced sensitivity of the sensor surface. An OCP decrease of 27 mV was observed when the gene copy number increased  $10^2$ -fold.

### **3.3. Design and fabrication of an integrated microfluidic system for LAMP reaction and solution-phase electrochemical detection**

This part shows that the platinum heater on the microfluidic chip operates stably and can be accurately calibrated. The measured temperature on the heater increased almost linearly with applied voltage, with a correlation coefficient  $r = 0.979$  and  $R^2 \approx 0.958$ , meaning that about 96% of the temperature variation is explained by the applied voltage. The regression equation  $*T = 12.26 + 3.137 \cdot V*$  allows the temperature to be inferred from the voltage with low error, which is very useful when operating the chip without attaching a separate temperature sensor to each reaction chamber.

Thus, it can be concluded that the design, material selection, and integration approach of the heater on the microfluidic system are appropriate, meeting the requirement for precise temperature control of the LAMP reaction while reducing the resources and the number of components needed in the experiment.

---

## CONCLUSION

The thesis “*Fabrication and Characterization of an Integrated Microfluidic System: Orientation towards Applications in Analysis and Material Synthesis*” has been carried out by the author and the following main results have been achieved:

(1) An experimental system has been successfully established for monitoring the DNA amplification of HBV virus by the LAMP reaction on a biochip. The entire process – from amplification to electrochemical signal analysis – is completed in less than 70 minutes.

(2) An rGO-PANi-based electrochemical sensor has been successfully fabricated for detecting amplified DNA products by open-circuit potential (OCP) measurement. The high conductivity of the rGO layer combined with the intrinsic pH sensitivity of PANi significantly enhances the overall sensitivity of the sensor surface; an OCP decrease of approximately 27 mV is observed when the gene copy number increases by  $10^2$ -fold.

(3) An integrated microfluidic system that performs both isothermal LAMP amplification and electrochemical detection on the same chip has been proposed and preliminarily completed. The integrated heater has been tested and operates stably, being able to reach and maintain the temperature range of 60–65 °C required for the LAMP reaction with a power supply of approximately 15–17 V.

## RECOMMENDATIONS

(1) Test the ability of the fabricated integrated device to detect biomarkers or pathogens using real clinical samples to determine its practical sensitivity and specificity.

(2) Test the device with multi-channel structures that allow simultaneous detection of multiple biomarkers in a single measurement and evaluate its response and stability.

(3) Further research combining 3D printing and screen-printed electrodes to simplify fabrication, optimise configuration and automation in sample preparation, as well as data acquisition and processing, moving towards a miniaturised lab-on-a-chip mode.

## **LIST OF THE PUBLICATIONS RELATED TO THE DISSERTATION**

1. Van Anh, N., Van Trung, H., Tien, B.Q. et al, Development of a PMMA Electrochemical Microfluidic Device for Carcinoembryonic Antigen Detection -. Journal of Elec Materi, 2016, 45: 2455.
2. Thu, V.T., Mai, A.N., Le The Tam et al., Fabrication of PDMS-Based Microfluidic Devices: Application for Synthesis of Magnetic Nanoparticles, Journal of Elec Materi, 2016, 45: 2576.
3. Tien, B.Q., Ngoc, N.T., Loc, N.T. et al., Biochip for Real-Time Monitoring of Hepatitis B Virus (HBV) by Combined Loop-Mediated Isothermal Amplification and Solution-Phase Electrochemical Detection, Journal of Elec Materi, 2017.
4. Thu, V.T., Tien, B.Q., Lam, T.D., Nga, D.T.N. et al., Reduced graphene oxide-polyaniline film as enhanced sensing interface for the detection of loop-mediated-isothermal-amplification products by open circuit potential measurement, RSC Adv., 2018, 8, 25361-25367.